Praktikum aus Neutronenphysik

The Magnetic Moment of the Neutron

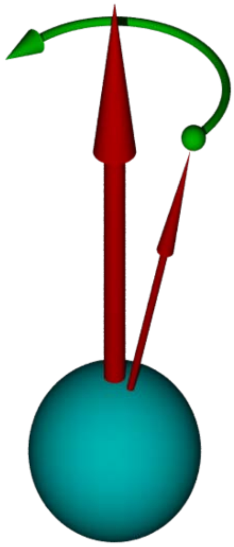

Ass. Prof. Dipl.-Ing. Dr.techn. Erwin Jericha

Associate Prof. Dipl.-Ing. Dr. Yuji Hasegawa

Dipl.-Ing. Armin Danner

download manual:

http://www.neutroninterferometry.com/home/teaching

Atominstitut
Technische Universität Wien
Stadionallee 2, 1020 Vienna, Austria

Sommersemester 2021

Contents

1 Introduction

1.1 Neutrons in magnetic fields: Larmor precession

The motion of a free propagating neutron, interacting with a magnetic field $\vec{B}(\vec{r},t)$ is described by a nonrelativistic Schrödinger equation, also referred to as *Pauli equation*, given by

$$\hat{H}\Psi(\vec{r},t) = \Big(-\frac{\hbar^2}{2m}\vec{\nabla}^2 - \mu\vec{\sigma}\vec{B}(\vec{r},t)\Big)\Psi(\vec{r},t) = i\hbar\frac{\partial}{\partial t}\Psi(\vec{r},t), \tag{1}$$

where m and μ are the mass ($1.6749\ 10^{-27}$ kg) and the magnetic moment ($-1.913\,\mu_{\mathrm{N}}$, with $\mu_{\mathrm{N}} = 5.051\ 10^{-27}$ J/T) of the neutron, respectively. $\vec{\sigma}$ is the Pauli vector operator. A solution is found by the two dimensional spinor wave function of the neutron, which is denoted as

$$\Psi(\vec{r},t) = \begin{pmatrix} \Psi_+(\vec{r},t) \\ \Psi_-(\vec{r},t) \end{pmatrix} = \phi(\vec{r},t)|S\rangle, \tag{2}$$

with spatial wave function $\phi(\vec{r},t)$. The state vector for the spin eigenstates denoted as $|\Uparrow\rangle$ and $|\Downarrow\rangle$ is given by

$$|S\rangle = \cos\frac{\vartheta}{2}|\Uparrow\rangle + e^{i\varphi}\sin\frac{\vartheta}{2}|\Downarrow\rangle, \tag{3}$$

introducing polar angle ϑ and azimuthal angle φ, which can be represented on a *Bloch sphere* or *Poincaré sphere*, as shown in Fig. 1. *Poincaré sphere* is usually used for the representation of light polarization. In the field of general two-level systems (qubits) the term *Bloch sphere* is conventionally used.

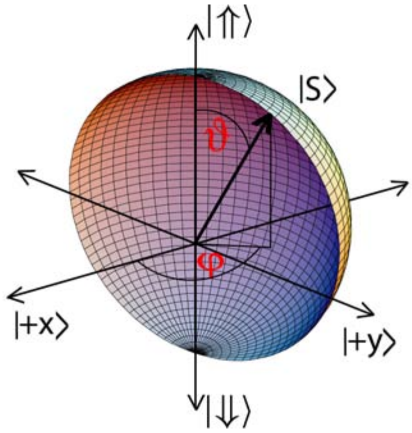

Figure 1: Bloch sphere description of arbitrary spin - $\frac{1}{2}$ state defined by polar angle ϑ and azimuthal angle φ.

The neutron couples via its permanent magnetic dipole moment $\vec{\mu}$ to magnetic fields, which is described by the Hamiltonian $H_{\mathrm{mag}} = -\vec{\mu}\cdot\vec{B} = -\mu\ \vec{\sigma}\cdot\vec{B}$. Magnetic fields of stationary and/or time dependent origin are utilized for arbitrary spinor rotations in neutron optics. When a neutron enters a stationary magnetic field region (non-adiabatically), the motion of its polarization vector, defined as the expectation value of the Pauli spin

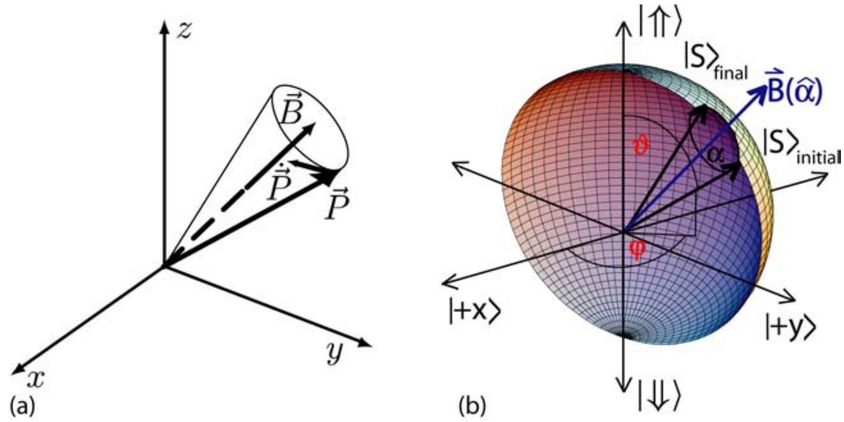

Figure 2: (a) Motion of polarization vector in real space: The polarization precedes about the direction of the external magnetic field, conserving the angle it embraces with the latter. (b) Bloch sphere description of precession of an arbitrary spin state defined by polar angle ϑ and azimuthal angle φ being transformed.

matrices $\vec{P} = \langle S|\vec{\sigma}|S\rangle$ is described by the Bloch-equation, exhibiting Larmor precession:

$$\frac{d\vec{P}}{dt} = \vec{P} \times \gamma\vec{B}, \tag{4}$$

where γ is a gyromagnetic ratio given by $2\mu/\hbar$. This is the equation of motion of a classical magnetic dipole in a magnetic field, which shows the precession of the polarization vector $\vec{P}$ about the magnetic field $\vec{B}$ with the Larmor frequency $\omega_{\mathrm{L}} = |2\mu B/\hbar|$. Details of the interaction of neutrons with magnetic field are given in http://www.neutroninterferometry.com/research-overview/neutrons-in-magnetic-fields-larmor-precession. The Larmor precession angle (rotation angle), solely depends on the strength B of the applied

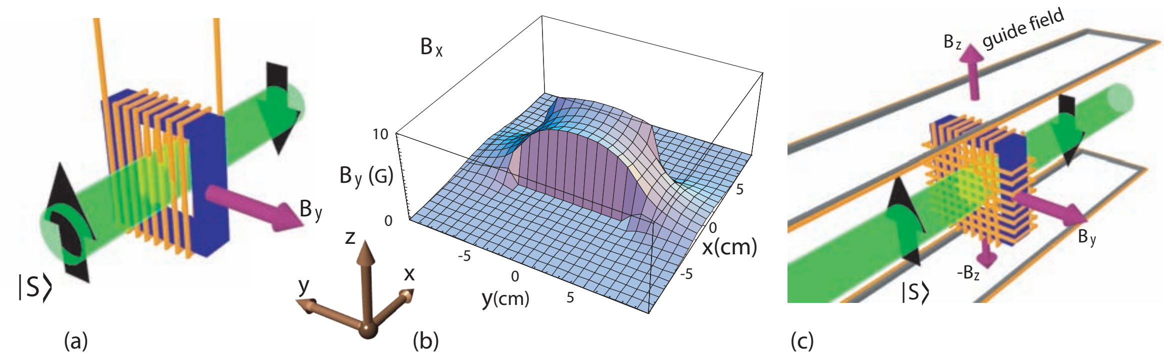

Figure 3: Direct Current (DC) spin-flipper (a) functional principle (b) Field configuration for highly non-adiabatic transition, required for Larmor precession (c) In practice a second coils ($-z$ direction), perpendicular to the original coil (x direction) is necessary to compensate the field component of the guide field ($+z$ direction).

magnetic field and the propagation τ within the field and is given by $\omega_L\tau$, as shown in Fig. (2) (a). Larmor precession is often utilized in co called Direct Current (DC) spin-rotators, or spin-flippers (if the spinor rotation angle is set to 180 deg). The illustrated field configuration assures a highly non-adiabatic transit required for Larmor precession. In practice a second coils ($-z$-direction), perpendicular to the original coil ($+x$-direction) is necessary to compensate the field component of the guide field ($+z$-direction), as illustrated in Fig. 3.

An oscillating RF field and a static magnetic field, denoted as $(0, B_1 \cos(\omega t + \phi))^T$, —a configuration used in nuclear magnetic resonance (NMR)—is also capable of spin flipping. Now we transform into a rotating frame which is rotating exactly at the Larmor frequency defined by the static field B_0, i.e., $\omega_{\mathrm{rot}} = \omega_{\mathrm{L}} = |\gamma B_0|$. The field in the rotating frame is given by $(0, B_1, B_0 + \frac{\omega_{\mathrm{rot}}}{\gamma}))^T$, where for $\omega_{\mathrm{rot}} = \omega_{\mathrm{L}} = |\gamma B_0|$ the static field component of magnitude B_0 is fully suppressed, which is called frequency resonance (the static component has to vanish, since we transformed into a rotating frame having exactly the Larmor frequency, a non zero static field would induce an additional Larmor precession which would conflict with the fact that we transformed into a frame rotating with Larmor frequency). If, in addition, the amplitude-resonance condition $B_1^{(\mathrm{res})} = \frac{\pi\hbar}{2\tau|\mu|} B_0$ — determining the amplitude of the rotating field — is fulfilled, a spin flip occurs.

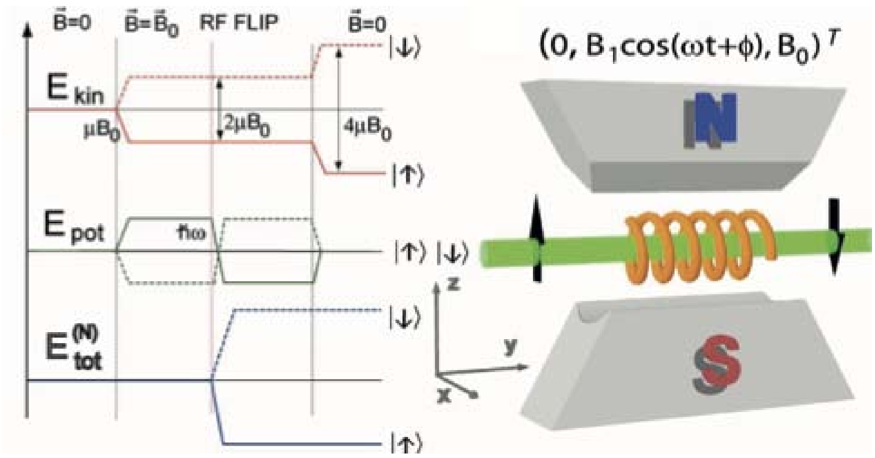

Figure 4: (right) RF-Flipper consisting of oscillating and perpendicular static magnetic field, (left) Energy diagramm.

1.2 Neutron polarimetry

A combination of two $\pi/2$-pulses (spin rotations) and an applied phase shift is generally referred to as *Ramsey interferometer* in NMR and atomic physics. In neutron optics a similar scheme is usually called polarimeter. A schematic illustration of a polarimeter is illustrated in Fig. 5 a. The first $\pi/2$ rotation creates a coherent superposition of the orthogonal spin eigenstates, by transforming the initial eigenstate, which is given by $|\Psi_{\mathrm{i}}\rangle = |\Uparrow\rangle$, according to

$$|\Psi_\mathrm{i}\rangle \xrightarrow{\pi/2} |\Psi'\rangle = 1/\sqrt{2}(|\Uparrow\rangle + |\Downarrow\rangle). \tag{5}$$

Before the second $\pi/2$ rotation probes it, a tunable phase shift (for example a static magnetic field) induces a phase shift ϕ:

$$|\Psi'\rangle \xrightarrow{\mathrm{PS}} |\Psi''\rangle = \frac{1}{\sqrt{2}}\Big(e^{-i\phi/2}|\Uparrow\rangle + e^{i\phi/2}|\Downarrow\rangle\Big) \equiv \frac{1}{\sqrt{2}}\Big(|\Uparrow\rangle + e^{i\phi}|\Downarrow\rangle\Big) \tag{6}$$

The probability of finding finally the system in $|\Uparrow\rangle$ ($|\Downarrow\rangle$) is given by $P_{\Uparrow,\Downarrow} = 1/2(1 \mp \cos\phi)$, which yields the well known sinusoidal intensity oscillations also depicted in Fig. 5 (a).

Neutron polarimetry has several advantages compared to for instance Mach-Zehnder (perfect crystal) interferometry, such as insensitivity to ambient mechanical and thermal disturbances, yielding high phase stability.

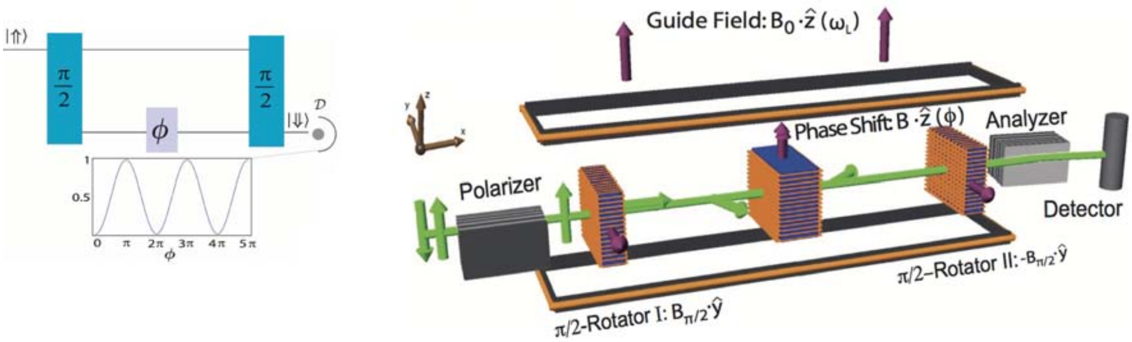

Figure 5: (a) Ramsey interferometer set-up, consisting of two indistinguishable paths. (b) Actual neutron polarimetric setup

2 Experimental Setup

2.1 Source & monochromator

Source

Fission of a ^{235}U nucleus in a **nuclear reactor** produces on average 2.5 fast neutrons, with energies around 1 MeV. This is more than needed to uphold the chain reaction. Therefore neutrons can be removed from the reactor for all kinds of experiments without disturbing the chain reaction. Since fast neutrons are not able to sustain a chain reaction, they have to be moderated by collisions with light nuclei of the moderator medium (e.g. protons in water). After this slowing down process the neutrons are denoted as *thermal* neutrons, with energies at about 25 meV, because they are in a thermal equilibrium with the moderating material. This concept can be used to produce neutrons in a variety of energies, depending on the temperature of the moderator.

The TRIGA MARK II reactor in Vienna (see Fig. 6) was installed by General Atomics in 1959, and went critical for the first time on march 7^{th} in 1962. The TRIGA reactor is a research reactor of swimming-pool type, used for **t**raining, **r**esearch and **i**sotope production (by **g**eneral **a**tomics = TRIGA). The TRIGA-reactor is a very common reactor type. Worldwide there are more than 50 TRIGA reactors in operation.

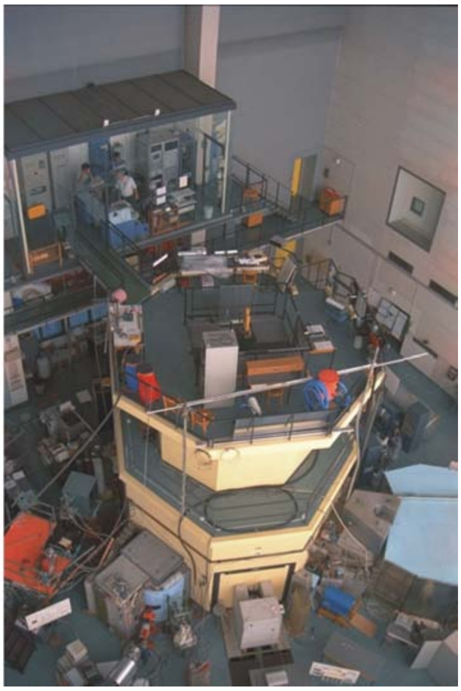

Figure 6: TRIGA MARK II reactor.

The reactor core consists of some 80 fuel elements that produce a maximum continous power output of 250 kW thermal. The heat is released via a primary (temperatures between 20 °C and 40 °C) and a secondary coolant circuit (temperatures between 12 °C and 18 °C). At nominal power the fuel temperature is about 200 °C. The fuel elements consist of a uniform mixture of 8 wt% uranium, 1 wt% hydrogen and 91 wt% zirconium. The zirconium-hydride is used as the main moderator. Since zirconium-hydride moderates, due to its negative temperature coefficient of reactivity, with less efficiency at high temperatures the reactor can be operated in pulse mode. At a pulse the power rises to 250 MW, which leads to an increase in the maximum neutron flux density of $1 \times 10^{13}\,\mathrm{cm}^{-2}\mathrm{s}^{-1}$ at 250 kW up to $1 \times 10^{16}\mathrm{cm}^{-2}\mathrm{s}^{-1}$ but only for 40 milliseconds. The reactor is controlled by three control rods containing boron carbide as absorber material. When the rods are fully inserted into the core all neutrons from the start-up source (a Sb-Be photoneutron source) are absorbed so that the reactor remains uncritical.

Monochromator

The experiment is carried out on the tangential beam tube of the TRIGA Mark II reactor, schematically depicted in Fig. 7. The out coming neutron beam is monochromatized by three mosaic crystals made of pyrolitic graphite, selecting the wavelengths 1.7 $\AA$, 2 $\AA$ and 2.7 $\AA$, the setup is located at the 1.7 $\AA$ beam line (*Bragg angle* 28.5°). The crystals yield high integrated reflectivity at low gamma radiation.

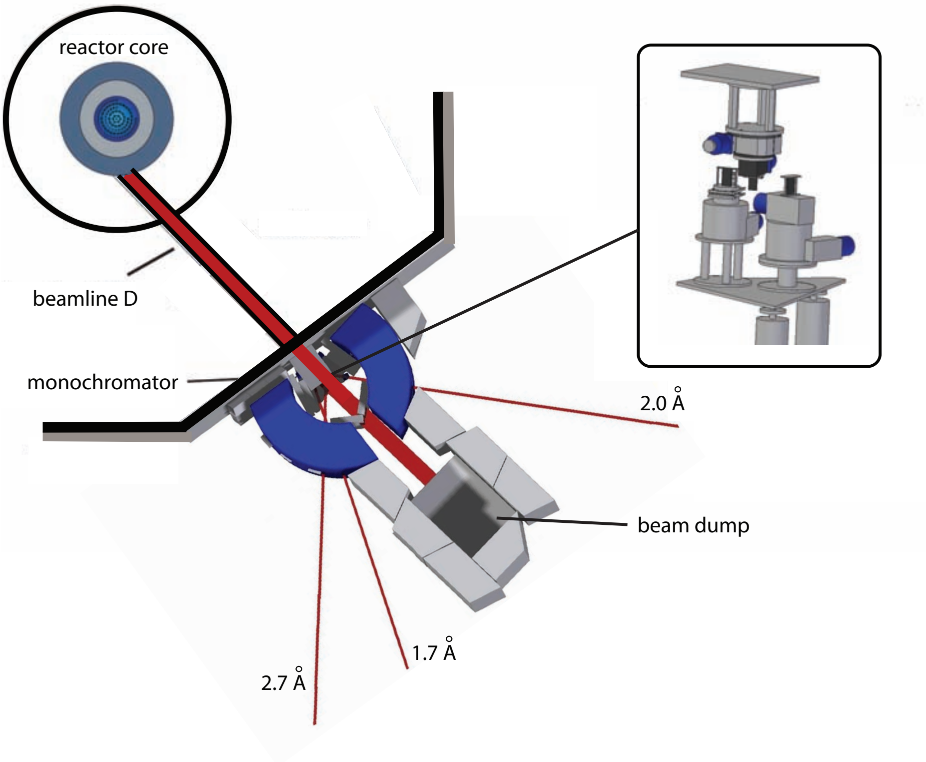

Figure 7: Tangential beam tube of the TRIGA Mark II reactor with monochromator.

2.2 Actual polarimeter setup

Polarizer/Analyzer

For understanding the mode of operation of the applied neutron polarizer we have to recap some basic concepts of neutron optics such as the refraction index. The time dependent Schrödinger equation $\nabla^2\Psi(\vec{r}) + K^2\Psi(\vec{r}) = 0$, with $K^2 = 2m/\hbar(E - V(\vec{r}))$ yields $n = K/k = \sqrt{1 - V(\vec{r})/E}$. From the strong (nuclear) interaction of the neutron we have the Fermi Pseudopotential denoted as $V_{\mathrm{nuc}}(\vec{r}) = \sum_i 2\pi\hbar^2 b_c/m\, \delta^3(\vec{r} - \vec{r}_i) \approx 2\pi\hbar^2 b_c N/m$, with the coherent scattering length b_c and the atom number density N (r_i denotes the position of each scattering center). From the magnetic interaction the contribution is given by $V_{\mathrm{mag}}(\vec{r}) = -\vec{\mu}\cdot\vec{B}_{\mathrm{eff}}$, with $\vec{\mu} = \mu\vec{\sigma}$, where μ is the magnetic moment of the neutron. So for materials containing Fe, Ni, or Co we have for the index of refraction $N_\pm(\vec{r}) = \sqrt{1 - (V_{\mathrm{nuc}}(\vec{r}) \pm \vec{\mu}\cdot\vec{B}_{\mathrm{eff}})/E}$. Since $V_{\mathrm{nuc}} \sim V_{\mathrm{mag}}$ n can become complex, which accounts for absorption or incoherent scattering. In general, we have $n < 1$ so the potential $V(\vec{r})$ is repulsive. For neutrons vacuum ($n = 1$) is an optically denser medium compared to most elements !

So neutrons are totally reflected if $E_\perp < V$. With $E_\perp = p^2/(2m) = 2\pi^2\hbar^2/(m\lambda_\perp)$ and $\lambda_\perp = \lambda/\sin\theta$ we get $\sin\theta < mV\lambda/(2\pi^2\hbar^2)$ and a critical angle $\theta_{\mathrm{crit}} = \arcsin\left(mV\lambda/\left(2\pi^2\hbar^2\right)\right)$, which is depicted in Fig 8 (a). For example Ni has a critical angle of $\theta^{\mathrm{Ni}}_{\mathrm{crit}} = 0.1\,°/\mathring{A}$.

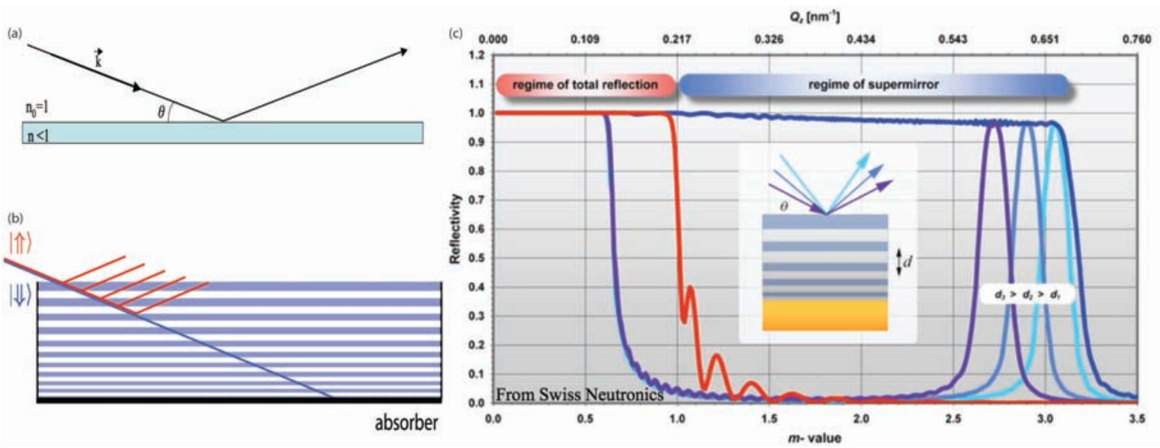

Figure 8: (a) neutron total reflection (b) spin-dependent reflection on multilayer structure. (c) supermirror specifications.

The polarizer and analyzer (spin filter) consists of a *multilayer* structure of two media A and B having different coherent scattering length $b_{c(A,B)}$. For an incident angle $\theta > \theta_{\mathrm{crit}}$ at every single boundary layer there will occur a transmitted an a reflected sub-beam. If the thickness of the layers is chosen in such way that the partial waves of the reflected sub-beams have an optical path difference of $n\lambda$; constructive interference will be observed. If the thickness of the layers varies only slightly, from layer to layer, there will be an appropriate "lattice constant" for a diversity of wavelengths. If alternating a **magnetic** and a **non-magnetic** medium is utilized, not only the nuclear scattering length, but also the magnetic scattering length has to be considered (see Fig 8 (b)). This can be used for beam polarization, since the sign of the magnetic scattering length depends of the orientation of the spin towards the magnetization of the medium. If a combination is chosen such that the sum of the nuclear scattering length and the magnetic scattering length for one spin component (for instance $|\Downarrow\rangle$) equals the scattering length of the non-magnetic substance, then this spin component will not be reflected, since there is no difference in the refractive index of the two layers for this spin component. However, the other spin component ($|\Uparrow\rangle$) will be (partly) reflected. The transmitted spin component ($|\Downarrow\rangle$) is absorbed after the last layer. An arrangement as discussed here is referred to as *supermirror*, often used as polarizer or analyzer. Supermirrors are characterized by their critical angle $m = \theta_{\mathrm{mirror}}/\theta_{\mathrm{Ni}}$, which is plotted in Fig 8 (c).

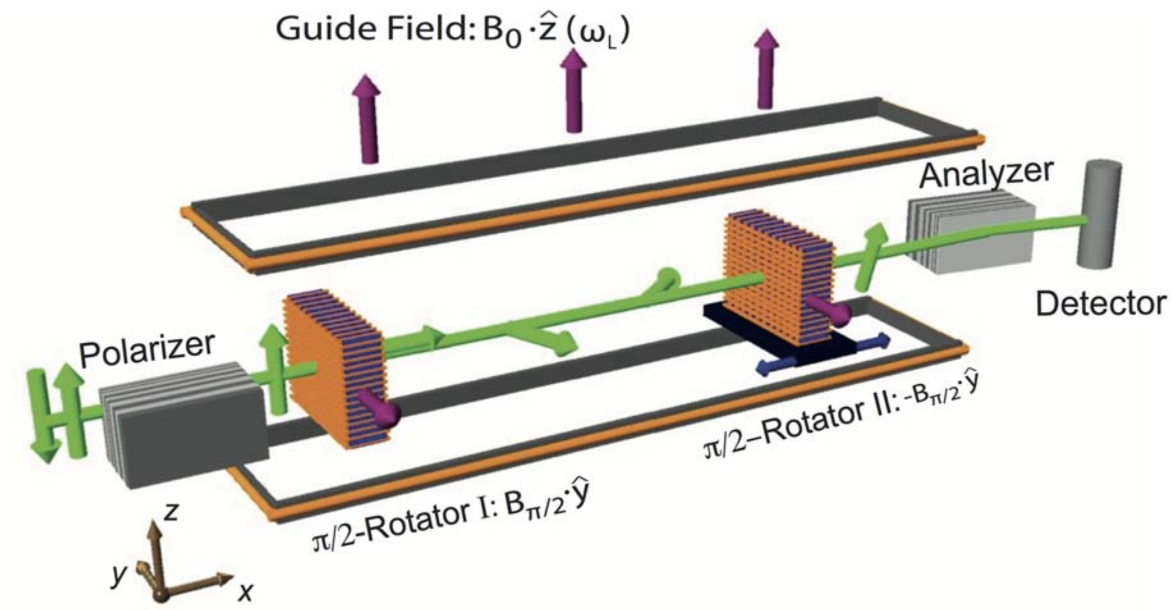

Figure 9: Schematic sketch of the experiment. A uniform guide field $B_0 \cdot \hat{z}$ is applied over the setup. The incident neutron beam is $|+z\rangle$-polarized by the supermirror polarizer. For a polarimetric measurement of this phase, the DC 1 converts the $|z\rangle$ state to $|x\rangle$ - a coherent superposition of the two spin eigenstates. Finally, in order obtain an intensity oscillation a translation δx of DC2, which projects the local $|x\rangle$ component back to $|z\rangle$, is performed.

Magnetic guide field

The entire setup is covered by a uniform guide field in Helmholtz configuration (pointing in $+z$-direction) to avoid depolarization during the passage of the setup (and to induce a Larmor precession to measure the magnetic moment of the neutron).

DC-coils

DC coils, as explained in Section 1.2, are used to rotate the spin. DC 1, with its field B_y is chosen such that it carries out a $\pi/2$ rotation around the y axis, generates a coherent superposition of the two orthogonal spin eigenstates, denoted as $|S'\rangle = 1/\sqrt{2}(|\Uparrow\rangle + |\Downarrow\rangle)$.

Detector

Since neutrons do not carry electrical charge they cannot be detected directly by ionization of a detector material. Neutrons can only be verified indirectly by measurement of charge, produced in a preceding nuclear reaction. The common method is to use **gas filled ionization chambers** where two electrodes, separated by a counting gas, collect the ion-pairs produced in a nuclear reaction. In a *BF_3-detector* the $^{10}_{5}$B nuclide is converted according to the following reaction

$$\mathrm{n} + {}^{10}_{5}\mathrm{B} \rightarrow {}^{11}_{5}\mathrm{B} \rightarrow \begin{array}{l} {\scriptstyle 93\%} \nearrow {}^{7}_{3}\mathrm{Li}* + {}^{4}_{2}\mathrm{He} \rightarrow {}^{7}_{3}\mathrm{Li} + {}^{4}_{2}\mathrm{He} + 2,31\ \mathrm{MeV} + \gamma(0,48\ \mathrm{MeV}) \\ {\scriptstyle 7\%} \searrow {}^{7}_{3}\mathrm{Li} + {}^{4}_{2}\mathrm{He} + 2,79\ \mathrm{MeV}, \end{array}$$

where the ionization is caused by the helium nuclei resulting in a detector pulse.

He-detectors use ^{3}He as filling gas, which has the advantage of a 40% higher absorption cross-section for neutrons. Hence it is possible to construct perspicuous smaller detectors, which results in better time resolution. The detector reaction is given by

$$\mathrm{n} + {}^{3}\mathrm{He} \rightarrow {}^{3}\mathrm{H} + \mathrm{p} + 0.764\ \mathrm{MeV}.$$

Scintillation counters absorb neutrons in a polymer or glass layer enriched with ^{6}Li or ZnS, which leads to a fluorescence radiation which is detected by a photo multiplier. Finally fission chambers use the n+^{235}U reaction for detection of neutrons. Since these detectors have a low counting probability, they are mainly used for monitoring applications. The setup used in the *Neutronen Praktikum* is equipped with a BF_3-detector.

2.3 DC-Coil handling

The tilt of a DC coil and produced magnetic field the B_y about the flight direction $+x$, can be detected by varying the magnetic field B_y (current scan) in the coil, which is depicted in Fig. 10. An intensity oscillation with roughly equal minima and zero offset, i. e. $\phi = \pi/2$, should be achieved. After adjusting the coil a symmetric intensity oscillation

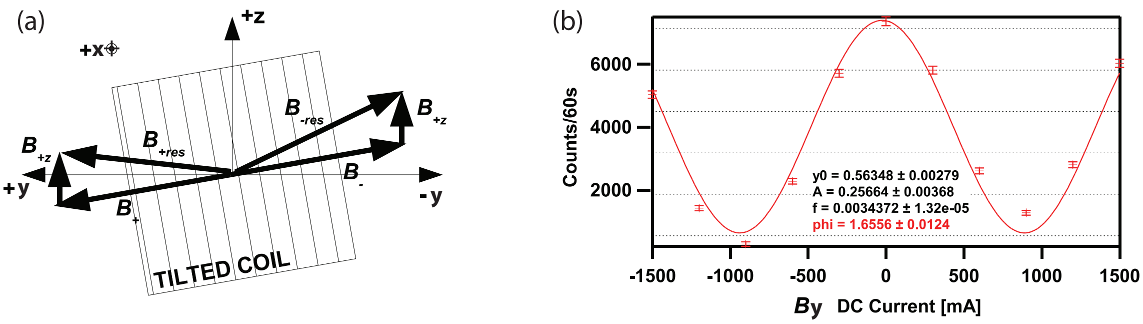

Figure 10: (a) Tilted DC coil (b) B_y Intensity scan.

with $\phi \sim \pi/2$ is observed, as depicted in Fig. 11. Without compensation field, the guide field, pointing in $+z$-direction, and the y-component of the coil add up to a field that cannot become perpendicular to the z-direction and therefore the incident up spin cannot be inverted from $|\Uparrow\rangle_z$ to the down stat $|\Downarrow\rangle_z)$ in the coil (Fig. 10 (a)). Hence a rather low flipping ratio, defined as $R = I_{\max}/I_{\min}$, is obtained.

The correct values for the guide field compensation are determined by choosing the current value that corresponds to one of the minima in the blue fit curve of Fig. 11 (b) for the y-field. With this y-current set, the current for the *compensation field* B_{-z} in the coil is varied.

The minimum intensity current of such a plot of the red curve shown in of Fig. 15 (a) is set and another y field variation is done, which is plotted in Fig. 15 (b). As a result, the flipping ratio $R = I_{\max}/I_{\min}$ increases significantly as well as the period of the measured oscillation. The minimum current from the B_y-scan, black curve in Fig. 15 (b), is used for

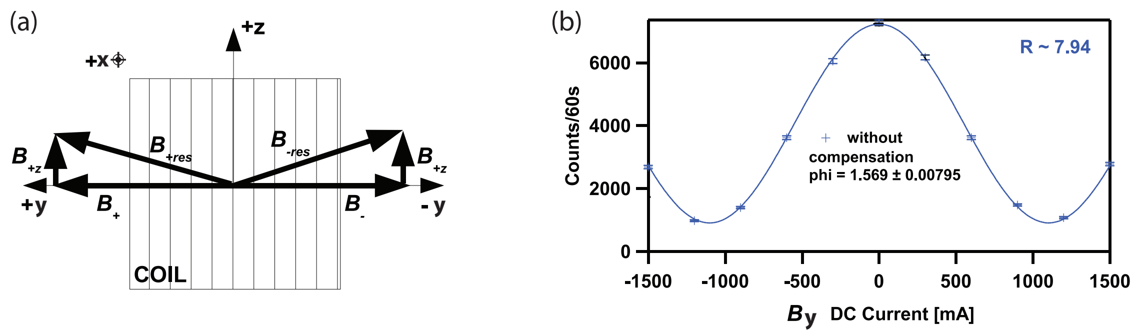

Figure 11: (a) Adjusted DC coil (b) B_y Intensity scan.

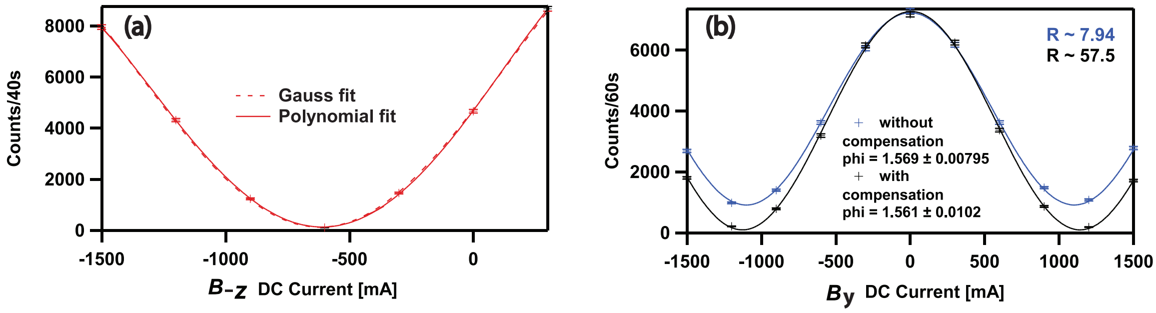

Figure 12: (a) Compensation field (B_{-z}) scan (b) B_y Intensity scan.

the spin flip configuration (π-rotation). For DC 1 (DC 4), which carries out a $\pi/2$-rotation, a quarter of the period of the curve is chosen.

2.4 Time-Of-Flight (TOF) Measurement

Time of flight (TOF) describes a variety of methods that measure the time that it takes for an (microscopic) object, particle or acoustic, electromagnetic or other wave to travel a certain distance. This measurement can be used for a time standard (such as an atomic fountain), or as a way to measure velocity a particle. Since neutrons are continuously

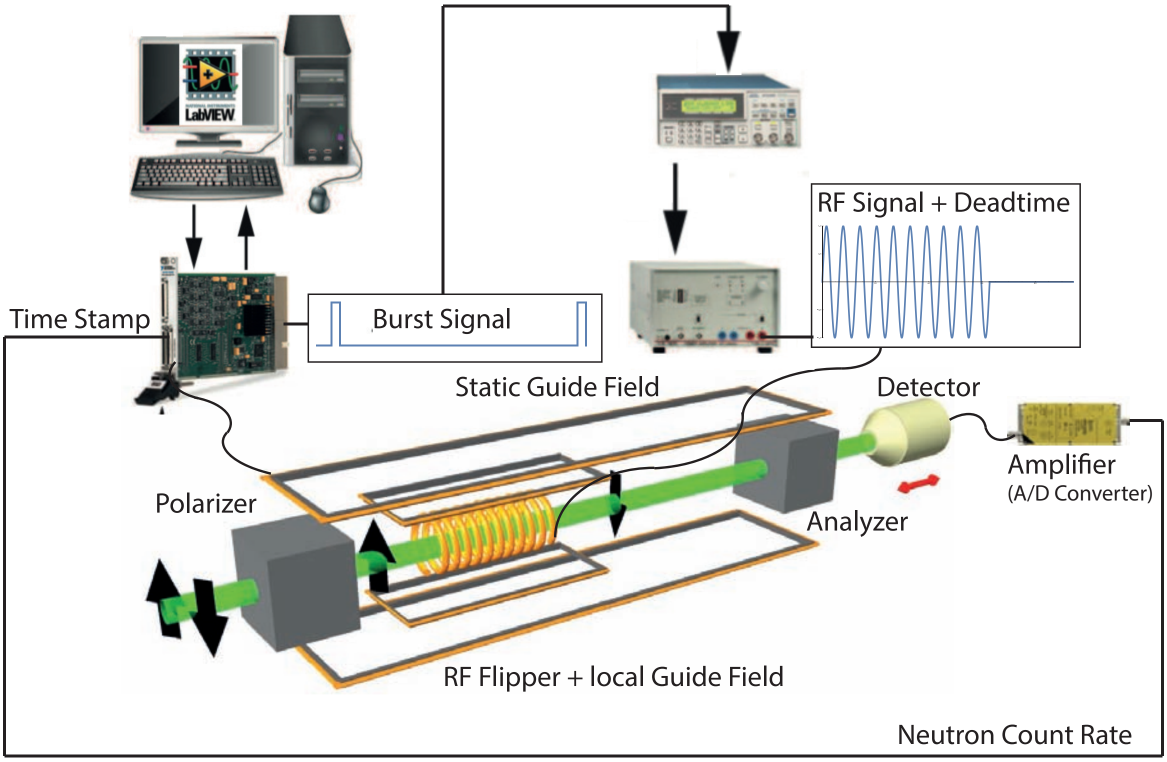

Figure 13: TOF-setup.

produced in the core of the reactor a periodic beam interruption has to inserted to have zero-time, which is synchronized with the detection system. This is usually realized using a mechanical beam chopper. However in our experiment we use a so called *spin-chopper* as schematically illustrated above.

When changing from *continouse* flipping mode to TOF the following steps have to be done:

- Change detector im putform counting card to FPGA card
- Connect *trigger* signal from FPGA card with signal generator (and osci)
- Set signal generator from *Continouse* to *Burst* mode
- Change signal generator trigger (Source) from *internal* to *external* via *Run Mode / Burst Parameters - MORE .../ Source / External*

- Set *N-Circles* of *Burst* mode between 10 and 15 (dependent on the chosen frequency such that half of the timing window is dead time)

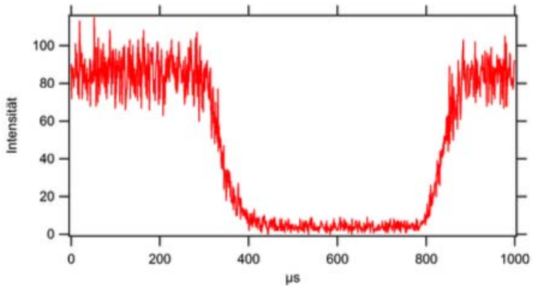

Figure 14: TOF-Signal: the neutrons that are between the end of the RF coil and the detector when the Rf field is switched on are not flipped.

RF-coils

An oscillating RF field and a static magnetic field, denoted as $(0, B_1 \cos(\omega t + \phi))^T$, —a configuration used in nuclear magnetic resonance (NMR)—is also capable of spin flipping. Now we transform into a rotating frame which is rotating exactly at the Larmor frequency defined by the static field B_0, i.e., $\omega_{\rm rot} = \omega_{\rm L} = |\gamma B_0|$. The field in the rotating frame is given by $(0, B_1, B_0 + \frac{\omega_{\rm rot}}{\gamma}))^T$, where for $\omega_{\rm rot} = \omega_{\rm L} = |\gamma B_0|$ the static field component of magnitude B_0 is fully suppressed, which is called frequency resonance (the static component has to vanish, since we transformed into a rotating frame having exactly the Larmor frequency, a non zero static field would induce an additional Larmor precession which would conflict with the fact that we transformed into a frame rotating with Larmor frequency). If, in addition, the amplitude-resonance condition $B_1^{(\rm res)} = \frac{\pi\hbar}{2\tau|\mu|} B_0$ — determining the amplitude of the rotating field — is fulfilled, a spin flip occurs.

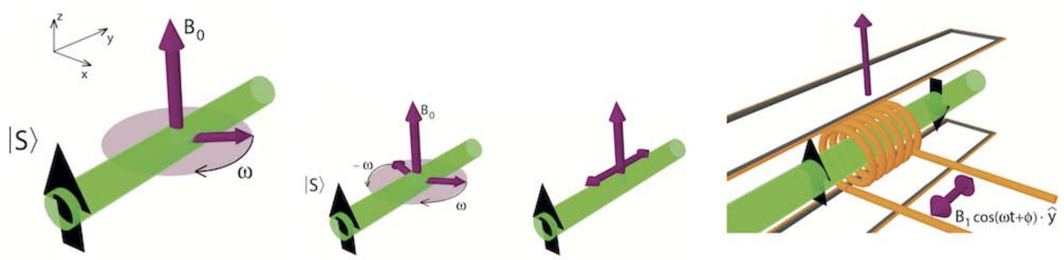

Figure 15: from left to right: i) rotating field, ii+iii) oscillating field, iv) RF spin flipper.

An oscillating RF field can be viewed as two counter-rotating fields. In the frame of one of the rotating components, the other is rotating at double-frequency and can be neglected (rotating-wave approximation). A consequence of the rotating-wave approximation is the so-called Bloch–Siegert shift, which gives rise to a correction term for the frequency resonance now reading $\omega_{\text{res}} = -\frac{2|\mu|}{\hbar\left(1+B_1^2/\left(16B_0^2\right)\right)}$. The above-explained combination of static and time-dependent magnetic fields is exploited in Radio Frequency (RF) flippers.

See http://www.neutroninterferometry.com/research-overview/neutrons-in-magnetic-field RF for details or **Appendix II**: Manipulating a Neutron Spin with a magnetic Field.

3 Experimental Procedure

- adjust DC 1 and DC 2, as explained in Section 2.3, to perform a π-flip: Repeat B_y-scans followed by tilting the coil until $\phi < \pm 1^\circ \rightarrow B_z$ - scan $\rightarrow B_y$ - scan $\rightarrow$ measure the flipping ratio with correct values for B_y and B_z. Prepare final plots of intensity vs B_y and B_z.
- measure the Larmor frequency (periode): DC 1 and DC are set to perform $\pi/2$ rotation. Wen the position of DC 2 is varied (using the micrometer screw) an intensity oscillations occurs due to different Larmor precession angles accumulated in the static magnetic guide field. Prepare a plot intensity vs. position of DC 2.
- measure the magnitude of the static guide field (using a Hall-probe).
- measure wavelength, more precisely the velocity, of the neutrons using the TOF-setup (explained in Section 2.4) by changing the position of the detector (using the micrometer screw) and comparing the time resolved intensity curves.
- calculate the magnetic moment of the neutron.

Appendix I: Properties of the Neutron

The neutron was discovered in 1932 by J.CHADWICK, an assistant of RUTHERFORD in Cambridge, during experiments that could be explained on the assumption that the incident radiation consisted of neutral particles of the mass of protons. The name results from the observation that the neutron does not pocess an electric charge. The fundamental significance of the neutron as part of the nucleus was first understood by W.HEISENBERG and D.IWANENKO only a short time later. Today, even the neutron's substructure, consisting of two down and one up quark (total charge: $\frac{2}{3}e^- + 2(-\frac{1}{3})e^- = 0$), is widely understood.

The neutron is a elementary particle with a mass of $m = 1.675.10^{-27}$ kg. It decays after a mean lifetime of $\tau = 889.1 \pm 1.8$ s into a proton, an electron and an antineutrino (β^--decay)

$$\mathrm{n} \longrightarrow \mathrm{p}^+ + \mathrm{e}^- + \bar{v}_e + 0.78\,\mathrm{MeV}. \tag{7}$$

The neutron carries a spin of $\frac{1}{2}$ which is accompanied by a magnetic dipole moment

$$\mu = -1.913\,\mu_{\mathrm{N}} \tag{8}$$

with $\mu_{\mathrm{N}} = 5.051\ 10^{-27}$ J/T, where μ_N is the nuclear magneton.

energy	
$\leq 10^{-5}$ eV	ultra cold
10^{-5} - 10^{-3} eV	cold
10^{-3} - 0,5 eV	thermal
$\geq$0,5 eV	hot

Table 1: Categories of neutrons.

Since the neutron carries *no charge* it can easily pass through condensed matter, even at very low energies. Due to this, neutrons are suitably used for radiography, which provides a very efficient tool for investigations in the field of non-destructive material testing. Despite the neutron's vanishing charge it carries a *magnetic dipole moment* which interacts with the domain structure of ferromagnetic solids. This method is called neutron depolarization analysis. It has developed into a powerful technique for investigation of domain structures of ferromagnetic materials. According to different wavelenght neutrons are separated into several categories as shown in Tab.(1).

Neutrons are subjected to all four fundamental forces. Since the neutron is part of the nucleus it is subjected to the *nuclear force*. The β-instability indicates that the neutron is also affected by the *weak force*. The neutron can interact *electromagnetically* via the magnetic dipole moment, and finally the finite mass of the neutron is responsible for interaction based upon *gravity*.

Appendix II: Larmor Precession - Neutron's Spin in a static magnetic Field

The temporal variation of an operator $\hat{A}$'s expectation value, is given by

$$\frac{\mathrm{d}}{\mathrm{d}t}\langle\hat{A}\rangle = \frac{\mathrm{d}}{\mathrm{d}t}\langle\psi|\hat{A}|\psi\rangle = \langle\dot{\psi}|\hat{A}|\psi\rangle + \langle\psi|\dot{\hat{A}}|\psi\rangle + \langle\psi|A|\dot{\psi}\rangle, \tag{9}$$

where the dot denotes quantities derived with respect to time. The derivatives of $|\psi\rangle$ and $\langle\psi|$ are given by the Schrödinger equation: $\hat{H}|\psi\rangle = \mathrm{i}\hbar|\dot{\psi}\rangle$, which gives $|\dot{\psi}\rangle = \frac{1}{\mathrm{i}\hbar}\hat{H}|\psi\rangle$ and $\langle\dot{\psi}| = -\frac{1}{\mathrm{i}\hbar}\langle\psi|\hat{H}$. This yields

$$\frac{\mathrm{d}}{\mathrm{d}t}\langle\hat{A}\rangle = -\frac{1}{\mathrm{i}\hbar}\langle\psi|\hat{H}\hat{A}|\psi\rangle + \langle\psi|\dot{\hat{A}}|\psi\rangle + \frac{1}{\mathrm{i}\hbar}\langle\psi|\hat{A}\hat{H}|\psi\rangle = \langle\psi|\dot{\hat{A}}|\psi\rangle + \frac{1}{\mathrm{i}\hbar}\langle\psi|[\hat{A},\hat{H}]|\psi\rangle, \tag{10}$$

which can be written as $\frac{\mathrm{d}}{\mathrm{d}t}\langle\hat{A}\rangle = \langle\frac{\partial\hat{A}}{\partial t}\rangle + \frac{1}{\mathrm{i}\hbar}\langle[\hat{A},\hat{H}]\rangle$, resulting in the Heisenberg equation, which describes the time dependent evolution of an operator's expectation value. It tells us that temporal changes in an operator's expectation value result from an explicit time dependence of the operator or its commutators with the constituents of the Hamilton operator of total energy. In reverse, the Heisenberg equation states that for a conserved quantity, denoted as $\hat{A}_{\mathrm{cons}}$, the corresponding operator must commute with the Hamiltonian $\hat{H}$: $\frac{\mathrm{d}}{\mathrm{d}t}\langle\hat{A}_{\mathrm{cons}}\rangle = \langle\frac{\partial\hat{A}_{\mathrm{cons}}}{\partial t}\rangle = 0$, from which immediately follows $[\hat{A}_{\mathrm{cons}},\hat{H}] = 0$.

In a next step the Heisenberg equation shall be applied to the the Pauli Spin operator $\vec{\sigma}$ from the Pauli equation, i.e., the Schrödinger equation for spin magnetic interaction

$$\hat{H}\Psi(\vec{r},t) = \big(-\frac{\hbar^2}{2m}\vec{\nabla}^2 - \mu\vec{\sigma}\cdot\vec{B}(\vec{r},t)\big)\Psi(\vec{r},t) = \mathrm{i}\hbar\frac{\partial}{\partial t}\Psi(\vec{r},t), \tag{11}$$

which consists of the neutron kinetic energy and the Zeeman magnetic energy given by $-\mu\vec{\sigma}\cdot\vec{B}(\vec{r},t)$. The equation of motion of the expectation value of the Pauli Spin operator hence is given by $\frac{\mathrm{d}}{\mathrm{d}t}\langle\vec{\sigma}\rangle = \frac{\mu}{\mathrm{i}\hbar}\langle[\vec{\sigma},\vec{\sigma}\cdot\vec{B}]\rangle$, with the commutator calculated as

$$\begin{aligned} -[\vec{\sigma},\vec{\sigma}\cdot\vec{B}] &= -\vec{\sigma}(\vec{\sigma}\cdot\vec{B}) + (\vec{\sigma}\cdot\vec{B})\vec{\sigma} \\ = -\sigma_i\sigma_j B_j + \sigma_i B_i\sigma_j &= -(\delta_{ij}\mathbb{1} + \mathrm{i}\epsilon_{ijk}\sigma_k)B_j + (\delta_{ij}\mathbb{1} + \mathrm{i}\epsilon_{ijk}\sigma_k)B_i \\ &= \mathrm{i}\epsilon_{ijk}\sigma_k B_j + \mathrm{i}\epsilon_{jki}\sigma_k B_i = 2\mathrm{i}(\vec{\sigma}\otimes\vec{B}) \end{aligned} \tag{12}$$

which gives $\frac{\mathrm{d}}{\mathrm{d}t}\langle\vec{\sigma}\rangle = \frac{\mu}{\mathrm{i}\hbar}\langle 2\mathrm{i}\vec{\sigma}\times\vec{B}\rangle = \frac{2\mu}{\hbar}\langle\vec{\sigma}\times\vec{B}\rangle = \gamma\langle\vec{\sigma}\times\vec{B}\rangle$, with γ being the gyromagnetic ratio. For a homogeneous magnetic fields (no spatial dependency) we have $\langle\vec{\sigma}\times\vec{B}\rangle = \langle\vec{\sigma}\rangle\times\langle\vec{B}\rangle$ and using the definition of the polarization vector $\vec{P} = \langle\vec{\sigma}\rangle$, we finally obtain

$$\frac{\mathrm{d}\vec{P}(t)}{\mathrm{d}t} = \vec{P}(t)\times\gamma\vec{B}, \tag{13}$$

which is the motion of the vector of polarization $\vec{P}$ in an homogeneous external magnetic field $\vec{B}$, which is referred to as Larmor precession.

Appendix III: Neutron Spin in an oscillating magnetic Field

For a combination of a rotating radio-frequency (RF), with a frequency ω, and a static magnetic field, in a configuration known from nuclear magnetic resonance (NMR), the magnetic field is denoted as $\vec{B}_{\mathrm{rot}}(t) = (B_1\cos(\omega t), B_1\sin(\omega t), B_0)^T$. The Pauli-Schrödinger equation for the neutron's wavefunction is given by

$$\mathrm{i}\hbar\frac{\partial}{\partial t}\Psi(x,t) = \big(-\frac{\hbar^2}{2m}\frac{\partial}{\partial x^2} - \mu\hat{\sigma}_x B_1\cos(\omega t) - \mu\hat{\sigma}_y B_1\sin(\omega t) - \mu\hat{\sigma}_z B_0\big)\Psi(x,t), \tag{14}$$

which is solved with a separation ansatz denoted as $\Psi(x,t) = \varphi(x)\psi(t) \equiv \varphi(x)\big(\psi_1(t), \psi_2(t)\big)^T$, where $\varphi(x)$ denotes the neutron's spatial wave function and $\psi(t)$ the (time dependent) spinor wave function in matrix notation. This yields

$$\mathrm{i}\hbar\frac{1}{\psi(t)}\frac{\partial}{\partial t}\psi(t) + (\mu B_1\,(\hat{\sigma}_x\cos(\omega t) + \hat{\sigma}_y\sin(\omega t)) + \mu B_0\hat{\sigma}_z) = -\frac{\hbar^2}{2m}\frac{1}{\varphi(x)}\frac{\partial^2}{\partial x^2}\varphi(x) \equiv C. \tag{15}$$

Both sides must be equal to a constant given by C, since the left side is only time depending and the right side only space dependent. The right side (only depending on the coordinate x), given by $\big(\frac{\partial^2}{\partial x^2} + \frac{2m}{\hbar^2}C\big)\varphi(x) = 0$, and its solution is a plane wave given by $\varphi(x) = \frac{1}{\sqrt{2\pi}}e^{\mathrm{i}\vec{k}\vec{r}}$, with $C = \frac{\hbar^2k^2}{2m}$.

However the spinor part remains much more complicated, where the equation

$$\mathrm{i}\hbar\frac{1}{\psi(t)}\frac{\partial}{\partial t}\psi(t) + (\mu B_1\,(\hat{\sigma}_x\cos(\omega t) + \hat{\sigma}_y\sin(\omega t)) + \mu B_0\hat{\sigma}_z) = \frac{\hbar^2k^2}{2m}, \tag{16}$$

can be transformed with the substitution $\psi(t) = \zeta(t)\exp\big(-\mathrm{i}\frac{\hbar k^2}{2m}t\big)$ to

$$\mathrm{i}\hbar\frac{\partial}{\partial t}\zeta(t) + \big(\mu B_1(\hat{\sigma}_x\cos(\omega t) + \hat{\sigma}_y\sin(\omega t)) + \mu B_0\hat{\sigma}_z\big)\zeta(t) = 0. \tag{17}$$

Now $\hat{\sigma}_+$ and $\hat{\sigma}_-$ are defined as $\hat{\sigma}_+ \equiv \hat{\sigma}_x + \mathrm{i}\hat{\sigma}_y$ and $\hat{\sigma}_- \equiv \hat{\sigma}_x - \mathrm{i}\hat{\sigma}_y$, which leads to

$$\mathrm{i}\hbar\frac{\partial}{\partial t}\zeta(t) + \Big(\frac{\mu B_1}{2}(\hat{\sigma}_+\exp(-\mathrm{i}\omega t) + \hat{\sigma}_-\exp(\mathrm{i}\omega t) + \mu B_0\hat{\sigma}_z\Big)\zeta(t) = 0. \tag{18}$$

Next a unitary transformation $\hat{U}(t)$ is introduced, which transforms the equation in a system rotating around the z-axis with a frequency of the magnetic field:

$$\zeta(t) = \hat{U}(t)\zeta_{\mathrm{rot}}(t) = \exp\big(-\mathrm{i}\frac{\omega t}{2}\hat{\sigma}_z\big)\zeta_{\mathrm{rot}}(t), \tag{19}$$

yielding

$$\begin{aligned}
&\frac{\hbar\omega}{2}\hat{\sigma}_z \exp\Big(-\mathrm{i}\frac{\omega t}{2}\hat{\sigma}_z\Big)\zeta_{\mathrm{rot}}(t) + \mathrm{i}\hbar\exp\Big(-\mathrm{i}\frac{\omega t}{2}\hat{\sigma}_z\Big)\frac{\partial}{\partial t}\zeta_{\mathrm{rot}}(t)\\
&+\Big\{\frac{\mu B_1}{2}\Big(\hat{\sigma}_+\exp(-\mathrm{i}\omega t)\exp\Big(-\mathrm{i}\frac{\omega t}{2}\hat{\sigma}_z\Big) + \hat{\sigma}_-\exp(\mathrm{i}\omega t)\exp\Big(-\mathrm{i}\frac{\omega t}{2}\hat{\sigma}_z\Big)\Big) +\\
&\mu B_0\exp\Big(-\mathrm{i}\frac{\omega t}{2}\hat{\sigma}_z\Big)\Big\}\zeta_{\mathrm{rot}}(t) = 0
\end{aligned} \tag{20}$$

When the equation is multiplied with $\exp\big(\mathrm{i}\frac{\omega t}{2}\hat{\sigma}_z\big)$ from the left side and the exponential function is expanded in a power series (with $\frac{\omega t}{2} = \alpha$) as

$$e^{\mathrm{i}\alpha\hat{\sigma}_z} = \mathbb{1} + \mathrm{i}\alpha\hat{\sigma}_z + \frac{(\mathrm{i}\alpha)^2}{2!}\hat{\sigma}_z^2 + \frac{(\mathrm{i}\alpha)^3}{3!}\hat{\sigma}_z^3 + ... \tag{21}$$

and using $\hat{\sigma}_i^2 = \mathbb{1}$ (with $i = x, y, z$)

$$e^{\mathrm{i}\alpha\hat{\sigma}_z} = \mathbb{1} + \mathrm{i}\alpha\hat{\sigma}_z + \frac{(\mathrm{i}\alpha)^2}{2!}\mathbb{1} + \frac{(\mathrm{i}\alpha)^3}{3!}\hat{\sigma}_z + ... = \begin{pmatrix} e^{\mathrm{i}\alpha} & 0 \\ 0 & e^{-\mathrm{i}\alpha} \end{pmatrix} \tag{22}$$

since

$$e^{\mathrm{i}\alpha} = \mathbb{1} + \mathrm{i}\alpha + \frac{(\mathrm{i}\alpha)^2}{2!} + \frac{(\mathrm{i}\alpha)^3}{3!} + ... \text{ and } \ e^{-\mathrm{i}\alpha} = \mathbb{1} - \mathrm{i}\alpha + \frac{(\mathrm{i}\alpha)^2}{2!} - \frac{(\mathrm{i}\alpha)^3}{3!} + ... \tag{23}$$

we get

$$\begin{aligned}
&\exp\Big(\mathrm{i}\frac{\omega t}{2}\sigma_z\Big)\sigma_z\exp\Big(-\mathrm{i}\frac{\omega t}{2}\sigma_z\Big)\\
&= \begin{pmatrix} e^{\mathrm{i}\alpha} & 0 \\ 0 & e^{-\mathrm{i}\alpha} \end{pmatrix}\begin{pmatrix} 1 & 0 \\ 0 & -1 \end{pmatrix}\begin{pmatrix} e^{-\mathrm{i}\alpha} & 0 \\ 0 & e^{\mathrm{i}\alpha} \end{pmatrix} = \begin{pmatrix} 1 & 0 \\ 0 & -1 \end{pmatrix} = \sigma_z.
\end{aligned} \tag{24}$$

In the same manner

$$\exp\Big(\mathrm{i}\frac{\omega t}{2}\sigma_z\Big)\hat{\sigma}_\pm\exp\Big(-\mathrm{i}\frac{\omega t}{2}\sigma_z\Big) = \exp\Big(\pm\mathrm{i}\omega t\Big)\hat{\sigma}_\pm. \tag{25}$$

This leads to the following simpler equation

$$\mathrm{i}\hbar\frac{\partial}{\partial t}\zeta_{\mathrm{rot}}(t) = \Big(-\frac{\hbar\omega}{2}\sigma_z - \frac{\mu B_1}{2}\underbrace{(\hat{\sigma}_+ + \hat{\sigma}_-)}_{2\sigma_x} - \mu B_0\sigma_z\Big)\zeta_{\mathrm{rot}}(t), \tag{26}$$

where the time dependency between the curly brackets has vanished. Now the following quantities are defined: $\omega_0 = -\frac{2\mu}{\hbar}B_0 = -\gamma B_0$ and $\omega_1 = -\gamma B_1$, which gives

$$\frac{1}{\zeta_{\mathrm{rot}}(t)}\frac{\partial}{\partial t}\zeta_{\mathrm{rot}}(t) = -\frac{\mathrm{i}}{2}\big((\omega_0\omega)\hat{\sigma}_z + \omega_1\hat{\sigma}_x\big), \tag{27}$$

where ω is the frequency of the rotating magnetic field, ω_0 is related to the guide field B_0 and ω_1 to the amplitude of the rotating field B_1, as introduced above. Integration leads to the following equation:

$$\ln \zeta_{\mathrm{rot}}(t) - \ln \zeta_{\mathrm{rot}}(0) = -\frac{\mathrm{i}}{2}\big((\omega_0 - \omega)\hat{\sigma}_z + \omega_1 \hat{\sigma}_x\big)t. \tag{28}$$

Since $\zeta_{\mathrm{rot}}(0) = \zeta(0)$ we get $\zeta_{\mathrm{rot}}(t) = \zeta(0)\exp\big(-\frac{\mathrm{i}}{2}\big((\omega_0-\omega)\hat{\sigma}_z + \omega_1\hat{\sigma}_x\big)t\big)$ and in the non rotating system a solution is calculated as $\zeta(t) = \zeta(0)\exp\big(\mathrm{i}\frac{\omega t}{2}\hat{\sigma}_z - \frac{\mathrm{i}}{2}\big((\omega_0-\omega)\sigma_z + \omega_1\hat{\sigma}_x\big)t\big)$. Using the definition $\vec{\alpha}(t) = (\omega_1 t, 0, (\omega_0-\omega)t)^T$ yields the final solution denoted as

$$\zeta(t) = \zeta(0)\exp\big(-\mathrm{i}\frac{\omega t}{2}\hat{\sigma}_z\big)\exp\big(-\mathrm{i}\vec{\sigma}\frac{\vec{\alpha}(t)}{2}\big), \tag{29}$$

with for instance $\zeta(0) = (1,0)^T$ accounting for an initial polarization pointing in $+z$-direction.

So far so good - the problem has been solved theoretically ! However what remains is to discuss the result and to understand its physical meaning. For this purpose, the second exponential has to be examined more precisely

$$\exp\Big(-\mathrm{i}\vec{\sigma}\frac{\vec{\alpha}(t)}{2}\Big) = \mathbb{1} - \mathrm{i}\vec{\sigma}\frac{\vec{\alpha}(t)}{2} + \frac{1}{2!}\Big(-\mathrm{i}\vec{\sigma}\frac{\vec{\alpha}(t)}{2}\Big)^2 + \frac{1}{3!}\Big(-\mathrm{i}\vec{\sigma}\frac{\vec{\alpha}(t)}{2}\Big)^3 + -..., \tag{30}$$

discussing the linear expressions sequentially, we obtain

$$\vec{\sigma}\frac{\vec{\alpha}(t)}{2} = \frac{1}{2}\big(\hat{\sigma}_x\omega_1 t + \hat{\sigma}_z(\omega_0-\omega)t\big) \tag{31}$$

for the linear term. For the quadratic term, since $\hat{\sigma}_x\hat{\sigma}_z + \hat{\sigma}_z\hat{\sigma}_x = 0$, we get

$$\Big(\vec{\sigma}\frac{\vec{\alpha}(t)}{2}\Big)^2 = \Big(\frac{\omega_1 t}{2}\Big)^2\mathbb{1} + \Big(\frac{(\omega_0-\omega)t}{2}\Big)^2\mathbb{1} = \Big(\frac{\vec{\alpha}(t)}{2}\Big)^2\mathbb{1}. \tag{32}$$

All together we finally obtain

$$\begin{aligned}\exp\Big(\mathrm{i}\vec{\sigma}\frac{\vec{\alpha}(t)}{2}\Big) &= \mathbb{1} - \mathrm{i}\vec{\sigma}\frac{\vec{\alpha}(t)}{2} - \frac{1}{2!}\Big(\frac{\vec{\alpha}(t)}{2}\Big)^2\mathbb{1} + \frac{1}{3!}\mathrm{i}\vec{\sigma}\frac{\vec{\alpha}(t)}{2}\Big(\frac{\vec{\alpha}(t)}{2}\Big)^2 + -... \\ &= \mathbb{1}\cos\frac{\vec{\alpha}(t)}{2} - \mathrm{i}\vec{\sigma}\vec{\alpha}_0(t)\sin\frac{\alpha(t)}{2},\end{aligned} \tag{33}$$

where we used $\sin(x) = x - x^3/(3!) + x^5/(5!) - +...$ and $\cos(x) = 1 - x^2/(2!) + x^4/(4!) - +...$, with the time-independent unit-vector calculated as

$$\vec{\alpha}_0(t) = \frac{\vec{\alpha}(t)}{|\vec{\alpha}(t)|} = -\frac{1}{|\vec{B}_{\mathrm{eff}}|}(B_1, 0, B_0 + \frac{\omega}{\gamma}) = -\frac{\vec{B}_{\mathrm{eff}}}{|\vec{B}_{\mathrm{eff}}|}, \tag{34}$$

with $|\vec{\alpha}(t)| \equiv \alpha(t) = t\sqrt{\omega_1^2 + (\omega_0-\omega)^2} = \gamma t\sqrt{B_1^2 + (B_0 + \frac{\omega}{\gamma})^2} \equiv \gamma t|\vec{B}_{\mathrm{eff}}|$.

In the rotating system, the neutron perceives the effective magnetic field $\vec{B}_{\mathrm{eff}}$.

In summary, the total wave function of the neutron can be expressed as

$$\Psi(x,t) = \varphi(x)\psi(t) = \frac{1}{\sqrt{2\pi}} \exp\Big(\mathrm{i}kx - \mathrm{i}\frac{\omega t}{2}\hat{\sigma}_z - \mathrm{i}\frac{\hbar k^2}{2m}t\Big)\Big(\mathbb{1}\cos\frac{\vec{\alpha}(t)}{2} - \mathrm{i}\vec{\sigma}\vec{\alpha}_0(t)\sin\frac{\alpha(t)}{2}\Big)\psi(0). \tag{35}$$

Using $\vec{\sigma}\vec{\alpha}_0 = -\vec{\sigma}\frac{\vec{B}_{\text{eff}}}{|\vec{B}_{\text{eff}}|} = -\frac{\hat{\sigma}_x B_1 + \hat{\sigma}_z(B_0+\omega/\gamma)}{|\vec{B}_{\text{eff}}|}$, and assuming the incident beam to be polarized in the z-direction, i.e., $\psi_0 = (1,0)^T$ and applying the Pauli matrices $\hat{\sigma}_x$, $\hat{\sigma}_z$ and the identity matrix $\mathbb{1}$ we finally get

$$\Psi(x,t) = \frac{1}{\sqrt{2\pi}} \exp\Big(\mathrm{i}\Big(kx - \frac{\hbar k^2}{2m}t\Big)\Big) \begin{pmatrix} \exp\Big(\frac{-\mathrm{i}\omega t}{2}\Big)\Big(\cos(\frac{\alpha(t)}{2}) + \mathrm{i}\frac{\mathrm{B}_0 + \frac{\omega}{\gamma}}{\mathrm{B}_{\text{eff}}}\sin(\frac{\alpha(t)}{2})\Big) \\ \\ \mathrm{i}\exp\Big(\frac{\mathrm{i}\omega t}{2}\Big)\frac{\mathrm{B}_1}{\mathrm{B}_{\text{eff}}}\sin(\frac{\alpha(t)}{2}) \end{pmatrix}, \tag{36}$$

which for $B_0 = B_1 = 0$ yields $\Psi(x,t) = \frac{1}{\sqrt{2\pi}}\exp\big(\mathrm{i}kx - \mathrm{i}\frac{E}{\hbar}t\big)(1,0)^T$, that is a free particle of energy $E = \frac{\hbar^2 k^2}{2m}$ polarized in $+z$ direction ($\vec{P} = \psi^*\vec{\sigma}\psi = (0,0,1)^T$).

If the rotating magnetic field has a resonance frequency $\omega \equiv \omega_{\text{res}} = \omega_0 = -\gamma B_0 = \omega_{\text{L}}$, the action of the static field B_0 is completely compensated and $\vec{B}_{\text{eff}} = (B_1, 0, B_0 + \omega/\gamma)^T$ has only a x-component. This condition is referred to as **frequency resonance**. At this point we would like to consider the z-component of the polarization given by $P_z = \psi^*\sigma_z\psi = \cos^2\frac{\alpha(t)}{2} + \frac{(B_o+\omega/\gamma)^2 - B_1^2}{(B_o+\omega/\gamma)^2 + B_1^2}\sin^2\frac{\alpha(t)}{2}$ which for frequency resonance reduces to $P_z^{\text{Freq Res}} = \cos^2\frac{\alpha(t)}{2} - \sin^2\frac{\alpha(t)}{2} = \cos(\omega_1 t)$. So if in addition the **amplitude resonance** for B_1, namely $t = \tau : \alpha(t) = \gamma\tau B_1 = -\pi \rightarrow B_1 = \frac{\pi\hbar}{2\tau|\mu|}$, with $\tau = L/v$ being is the transmission time through the dynamical spin flipper with a flipper length L, depending on the velocity v of the neutron, is fulfilled we get $P_z^{\text{Freq, Ampl Res}} = (0,0,-1)$; a spin flip occurred ! If we now calculate the wave function after the spin flip we get

$$\Psi(\tau) = \frac{1}{\sqrt{2}}e^{\mathrm{i}(kx - E/\hbar\, t)}\begin{pmatrix} 0 \\ \mathrm{i}e^{\mathrm{i}\omega_{\text{res}}/2} \end{pmatrix} = -\mathrm{i}\frac{1}{\sqrt{2}}e^{\mathrm{i}(kx - (E - |\mu|B_0)/\hbar\, t)}\begin{pmatrix} 0 \\ 1 \end{pmatrix}, \tag{37}$$

with $\vec{P} = \psi^*\vec{\sigma}\psi = (0,0,-1)^T$, that is polarization in $-z$-direction. One can immediately see that compared to the total energy before the spin flipp, given by $E_0 + |\mu|B_0$ the neutron hast lost an amount of energy $\Delta E = 2|\mu|B_0 = \hbar\omega_{\text{res}}$, by emission of a photon of frequency $\nu = \omega_{\text{res}}/(2\pi)$. In case of a flip from $(0,1)^T$ to $(1,0)^T$ the neutron absorbs an photon of the same energy from the rf-field.

For a oscillating field with phase of form $\vec{B}(t) = \begin{pmatrix} B_1\sin(\omega t + \phi) \\ B_1\cos(\omega t + \phi) \\ B_0 \end{pmatrix}$ the effective field in frequency resonance reads $\vec{B}_{\text{eff}} = \begin{pmatrix} B_1\sin(\phi) \\ B_1\cos(\phi) \\ 0 \end{pmatrix}$.

However, in practice an oscillating field is used instead of a rotating one (though it is in principle feasible to implement a rotating filed). An oscillating field of frequency ω plus static magnetic guide field, denoted as $\vec{B}_{\text{osc}}(t) = (0, B_1^{\text{osc}}\cos(\omega t + \phi), B_0)^T$, can be

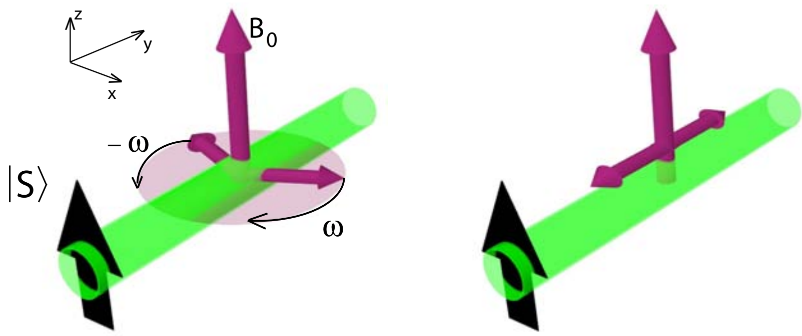

Figure 16: Graphical representation of an oscillating magnetic field decomposed in two counterrotating fields. Each of the rotating fields has half amplitude compared to the oscillating field.

decomposed as the sum of two counter-rotating fields with frequencies ω:

$$\vec{B}_{\text{osz}} = \begin{pmatrix} 0 \\ B_y \cos(\omega t) \\ B_0 \end{pmatrix} = \vec{B}_{\text{osz}} = \vec{B}_{1\,\text{rot}} + \vec{B}_{2\,\text{rot}}$$

$$= \begin{pmatrix} \frac{B_y}{2} \sin(\omega t + \phi) \\ \frac{B_y}{2} \cos(\omega t + \phi) \\ \frac{B_0}{2} \end{pmatrix} + \begin{pmatrix} \frac{B_y}{2} \sin(-\omega t + \phi) \\ \frac{B_y}{2} \cos(\omega t + \phi) \\ \frac{B_0}{2} \end{pmatrix}. \quad (38)$$

The interaction representation used above describes the physics in a rotating frame with the field component ? with the Larmor precession of the spin in the static field. The other component is seen in this frame as a fast rotating field (2ω), whose effect can be neglected, which is referred to as rotating wave approximation (RWA). A consequence of the rotating wave approximation is the so called Bloch Siegert shift, which originates from the second term 2. In 1940 Bloch and Siegert proved that the dropped part, oscillating rapidly, can give rise to a shift in the true resonance frequency such that $\omega_{\text{res}} \neq \omega_{\text{L}}$. Now the frequency resonance is given by $\omega_{\text{res}} = \frac{2|\mu|}{\hbar}\left(1 + \frac{B_1^2}{16B_0^2}\right)$ and the amplitude becomes $B_1^{\text{osc}}(t) = 2B_1^{\text{rot}}(t) = \frac{\pi\hbar}{\tau|\mu|}$.